Late Pleistocene and Holocene palaeoclimate, glacier and treeline reconstruction based on geomorphic evidences in the Mongun-Taiga massif (south-eastern Russian Altai)

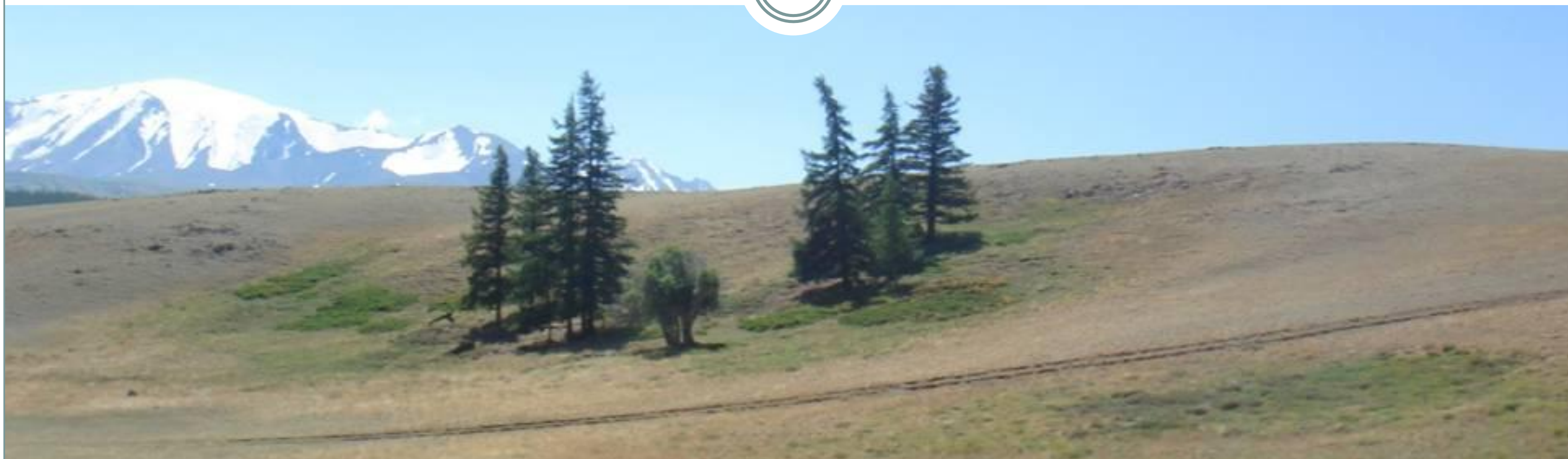

Dmitry Ganyushkin[a], Kirill Chistyakov[a], Ilya Volkov[a], Dmitry Bantcev[a], Elena Kunaeva[b], Dagmar Brandová[c], Gerald Raab[c], Marcus Christl[d], and Markus Egli[d]

[a]Saint-Petersburg State University, Russian Federation
[b]Pushkin Leningrad State University, St Petersburg (Pushkin), Russian Federation
[c]Department of Geography, University of Zurich, Zurich, Switzerland
[d]Laboratory of Ion Beam Physics, ETH Zurich, Switzerland

1.The area of research

Orographic map of the Mongun-Taiga massif and neighbouring mountain ranges with the insert in the upper left showing the study area on the Eurasian continent.

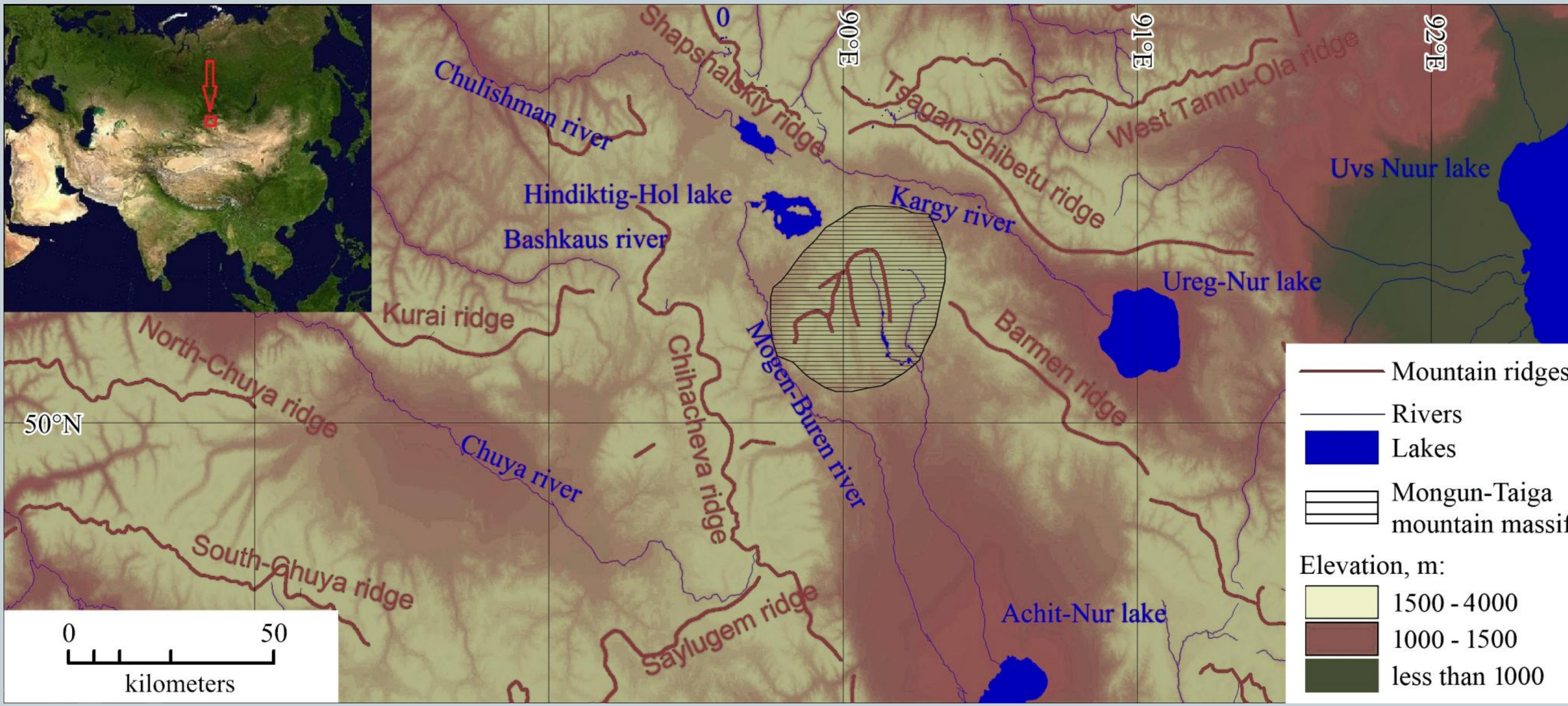

The Mongun-Taiga mountain massif is situated in the south-eastern periphery of the Russian Altai mountains . It is located within the internal drainage basin of the Mongolian Great Lakes. The highest peak has an elevation of 3971 m *a.s.l.*

Climate and upper treeline

The climate of the massif is cold and arid. According to data of the closest meteorological station Mugur-Aksy (1830 m *a.s.l.*, 50° 22′ 45″ N, 90° 26′ 0″ E; WMO code 362780: about 30 km to the north-east of the massif) the average annual precipitation is 160 mm, the mean summer temperature is 12.0 °C and mean temperature about – 3 °C. Forest vegetation is concentrated on the northern slopes of the massif with *Larix Sibirica* usually occurring between 2000 and 2400 m *a.s.l.* The upper treeline varies between 2400 m on north-western slopes to 2300 on the north-eastern slopes. The upper treeline of the north-eastern slopes corresponds to an average summer temperature of 8.8 °C (Chistyakov et al., 2012).

Glaciers

Currently, there are 30 glaciers having a total area of 20.2 km^2 within the massif. Valley glaciers comprise over half of that area. The number of small hanging and cirque glaciers, however, is also significant. Usually, the largest glaciers develop on the leeward, north-eastern slopes. The vertical extension of glaciation is from 3970 to 2900 m *a.s.l.* The average ELA for the glaciers of the Mongun-Taiga massif is at 3390 m *a.s.l.*

The area is remote and there are almost no roads

2. Methods

Glacier observations

Spot-5 21-07-2014 space image, fragment

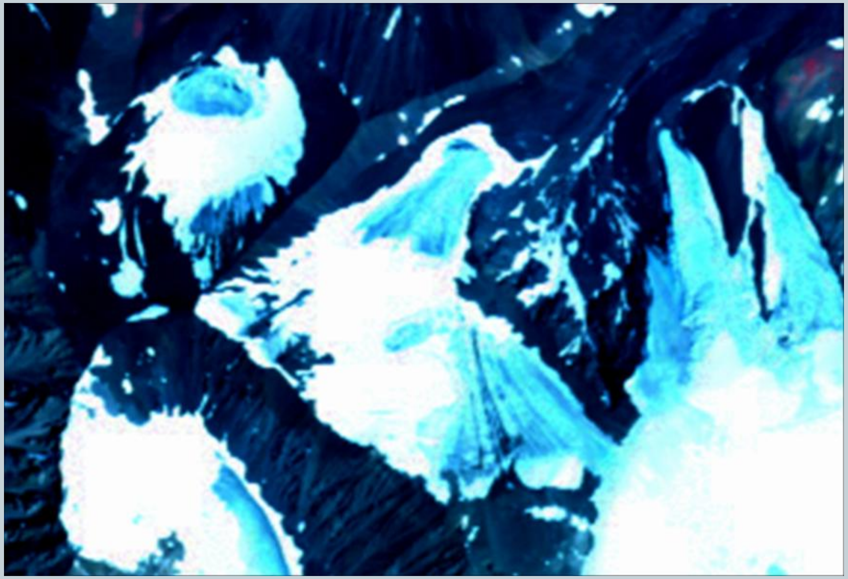

Include the geodetic surveys (Leviy Mugur glacier and its LIA moraine (in 1994), the snout and LIA moraines of the Shara-Horagai glacier (1990, 2013), the East Mugur (2012); aerial photo and space imagery analysis (Landsat-7 04.09.2001, Landsat-8 12.08.2013, Spot-5 2011-09-19, Spot-5 21-07-2014). The imagery was orthorectified using the 30 m ASTER GDEM v.2 digital elevation model (https://gdex.cr.usgs.gov/gdex/). The delineation of the glaciers and moraines was mapped manually. The minimum size of glaciers to be mapped was 0.01 km^2. The boundary line was mostly determined by direct observations. The determination of the present-day ELA of the Mongun-Taiga was performed by using by direct observations (at the end of the ablation season during several years) and satellite imagery at the end of the ablation seasons.

Geomorphic observations

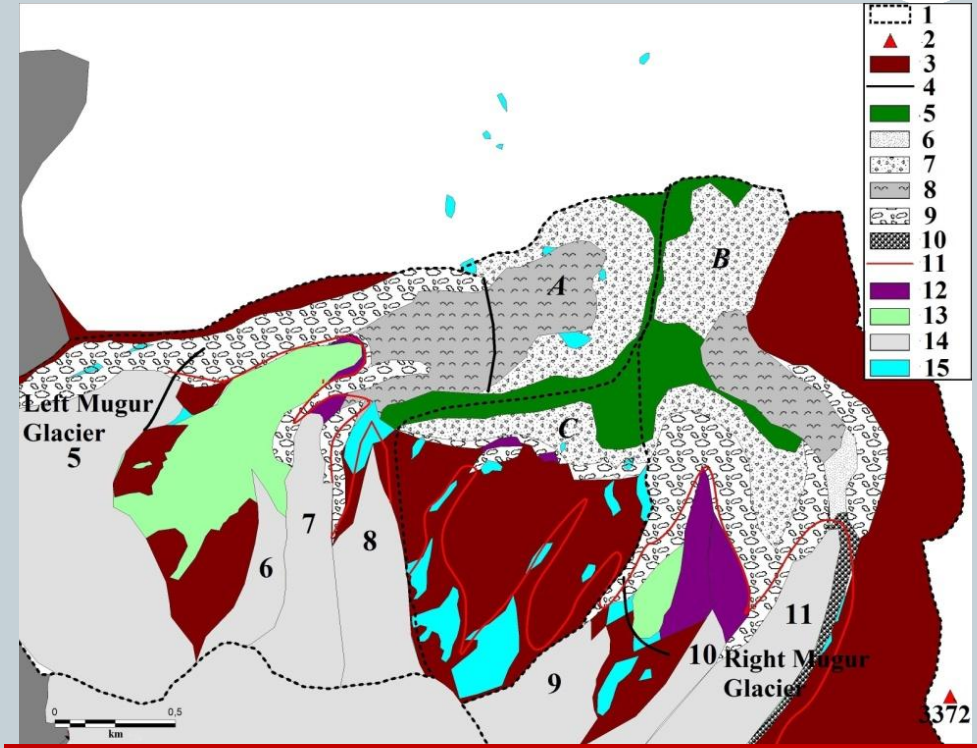

Glacial complexes Left Mugur (A), Right Mugur (B), Central Mugur (C)

Legend: 1- borders of the complexes, 2- mountain tops, 3- steep rocky slopes, 4- rigels, 5- intermorainal depressions and eroded moraine, 6- glacier outwash plain, 7- historical stage moraines, 8- rock glaciers, 9- LIA moraines, 10- the former medial moraine, 11- glaciers at 1966, 12- debris-covered ice formed in 1966-1995, 13- debris-covered ice formed in 1995-2008,14- present glaciers (with numbers from catalogue), 15- present perennial snow patches

The following glacio-geomorphic features were mapped: cirques, riegel, troughs, trough shoulders and moraine ridges. This mapping resulted in the reconstruction of the position and margins of former glaciers. Parameterisation of the present and reconstructed glaciers was performed using topographic maps at a scale of 1:100000 and 1:25000.

Meteorological and hydrological observations

Observations were done in the Shara-Horagai (1990, 2013; 3130 *m a,s.l.*; 2780 *m a.s.l.;* 3800 *m a.s.l.*), Vostotschniy (East) Mugur (1993, 1995, 2010, 2011, 2012; 2259 *m a.s.l.*, 2668 *m a.s.l.*) and the Praviy Mugur (1994; 3200 *m a.s.l.*, 2610 *m a.s.l.*) observation stations. In each case, measurements (air and ground temperature, precipitation, solar radiation, air humidity) were continuously done during the ablation season at different elevational points: close to the upper treeline; near the edges of glaciers; on glacial surfaces; on lateral moraines over the glacial snouts and on the main summit of the massif. In addition, the data of the Mugur-Aksy meteorological station were considered. Using all these datasets, a spatial extrapolation and modelling was rendered possible.

Relative dating of surfaces

Relative-dating techniques based on weathering patterns were used to delineate a chronology of moraines. On a polygon (moraine) having an area of 100 m^2, boulders having a diameter over 30 cm were marked and counted. Then properties were measured that included the occurrence of shear-strained boulders (C, %), the degree of embedment into finely-grained material (B, %), weathering rind measurements (W, mm), lichen coverage (L, %), the number of boulders having a diameter over 30 cm (N), rock surface hardness (R) and the proportion of flat-topped boulders (F, %). The rock surface hardness was measured using a Schmidt hammer, which measures the rebound value of a boulder and is a portable instrument originally developed to test concrete quality in a non-destructive way A spring-loaded bolt impacting a surface yields a rebound- or R-value, which is proportional to the hardness (compressive strength) of the rock surface. More-weathered surfaces provide low R-values and less-weathered surfaces correspondingly high R-values. Three measurements were done for each boulder (5 when there were larger differences between individual measurements) and then the average value was registered. Measurements were carried out at 19 sites where about 2500 boulders were described and analysed.

Numerical dating of surfaces

Dating of buried wood samples, peat and soils (humus) was done using the radiocarbon technique. Peat and wood samples were cleaned using an acid-alkali-acid (AAA) treatment. ^{14}C dating was performed at the KÖPPEN-Laboratory of the Saint-Petersburg State University. Radiocarbon dating was performed by using a Quantulus 1220 liquid scintillation spectrometer (Perkin Elmer, USA). Dating of strongly-decomposed peat and humus (palaeosoils) was performed on the fraction that dissolves in hot 2 % NaOH (Arslanov et al., 1993). A V_2O_5 coated $Al_2O_3 \times SiO_2$ catalyst has been employed for benzene synthesis.

The calendar ages were obtained using the OxCal 4.3 calibration program (Bronk Ramsey, 2001, 2009) based on the IntCal 13 calibration curve (Reimer et al., 2013). Calibrated ages are given in the 1s range (minimum and maximum value for each). If not otherwise mentioned in the text, calibrated years BP (cal BP) are used.

We also did some dating of rock boulders using ^{10}Be. However, the suitability of rock boulders was very limited. Two small boulders (c. 0.3 m in height) were sampled and analysed for in situ ^{10}Be. The rock samples were pre-treated following the standard procedures. The $^{10}Be/^{9}Be$ ratios were measured at the ETH Laboratory Ion Beam Physics' Accelerator Mass Spectrometry (AMS) facility using the ^{10}Be standard S2007N with a nominal value of $^{10}Be/^{9}Be = 28.1 \times 10^{-12}$

ELA and palaeoclimate modelling

- Modelling of palaeotemperature, palaeoprecipitation and ELA was done using the approach of Ganyushkin (2015) and Glazyrin (1985) according to which the changes of the ELA **(**$\Delta Z_o = Z_{on} - Z_o$**)** *as a result of climate chenge* are given by:

1) $$\Delta Z_0 = -(P \cdot c(Z_0) - a(T(Z_0) + \Delta T))/(E_n)$$

where $c(Z_o)$ = present accumulation at the ELA; P = ratio of past annual precipitation to present-day situation; T = mean summer temperature; a = ablation; $a(T(Z_o)+\Delta T)$ = ablation at the present-day ELA in case of a change of the average summer temperature ΔT; E_n = energy of glacierisation (activity indexor altitudinal mass balance gradient) under new climatic conditions.

The ablation at the ELA is calculated using the extrapolated data from the Mugur-Aksy meteorological station temperature (gradient 0.69 °C/100 m)) and the empiric regional formula (Chistyakov et al., 2012)^

2) $$a_i = 36{,}14(t_0)^2 + 294{,}6t_0 + 511{,}6$$

- At the ELA, ablation equals accumulation. The energy of glaciation (E_n) can then be calculated by

3) $$E = PK(\Delta p/\Delta Z) + \Delta a/\Delta Z$$

- where K = coefficient of snow concentration (at ELA), p = average annual precipitation at ELA, $\Delta p/\Delta Z$ = gradient of precipitation, $\Delta a/\Delta Z$ = gradient of ablation.

ELA and palaeoclimate modelling

- Equation 1) contains 3 variables: ΔZ_o, P, ΔT. The first of them can be derived from palaeoglacial reconstructions. The reconstruction of the ELA was done using the method proposed by Kurowsky (1891): 4) $z_{0n} = (z_0 S + \Delta S(z_1 + z_2)/2)/(S + \Delta S)$
- where z_{on}= reconstructed ELA, ΔS= difference between the area of the palaeoglacier and its present-day area, z_1= present-day altitude of the glacial snout and z_2= altitude of the palaeoglacial snout.
- With an estimation of ΔZ_o for the reconstructed glaciers, equation 1) can be used to determine P (if we know ΔT) and ΔT (if P is known). Using this approach, scenarios can be calculated by assigning a value to one of the unknown parameters.
- The choice of probable scenarios can be done on the basis on regional palaeoclimatic reconstructions or on regional statistical correlations between precipitation and temperature. In the south-eastern Altai there is a clear correlation between summer precipitation and average summer temperature (Ganyushkin, 2015), expressed by the following empirical equation:

5) $$\Delta T = 2.245 \ln P - 0.9779$$

- Another possibility is to use the correlation of monthly precipitation with monthly temperature from the closest meteorological station Mugur-Aksy to Mongun-Taiga massif (Ganyushkin, 2015). The empirical relationship looks as follows:

6) $$P = 0.6635 e^{0.0748 \Delta T}$$

Results

Moraine group 0

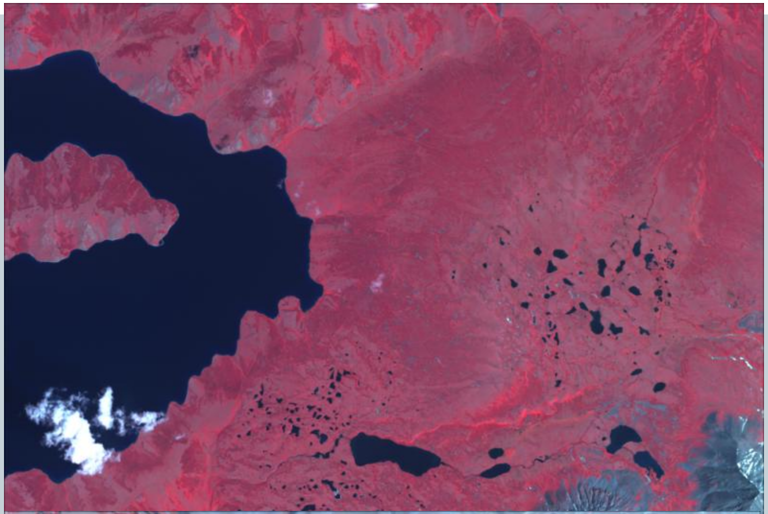

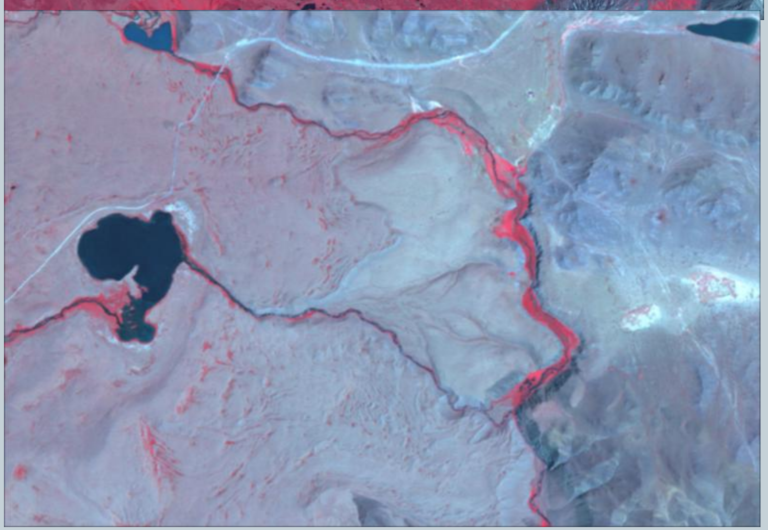

Such moraines are very smooth and weathered, they are fragmentary and were not used in our reconstructions

Moraine group I

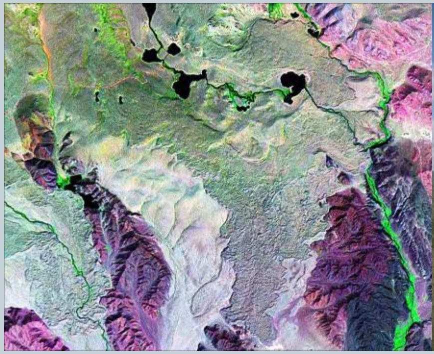

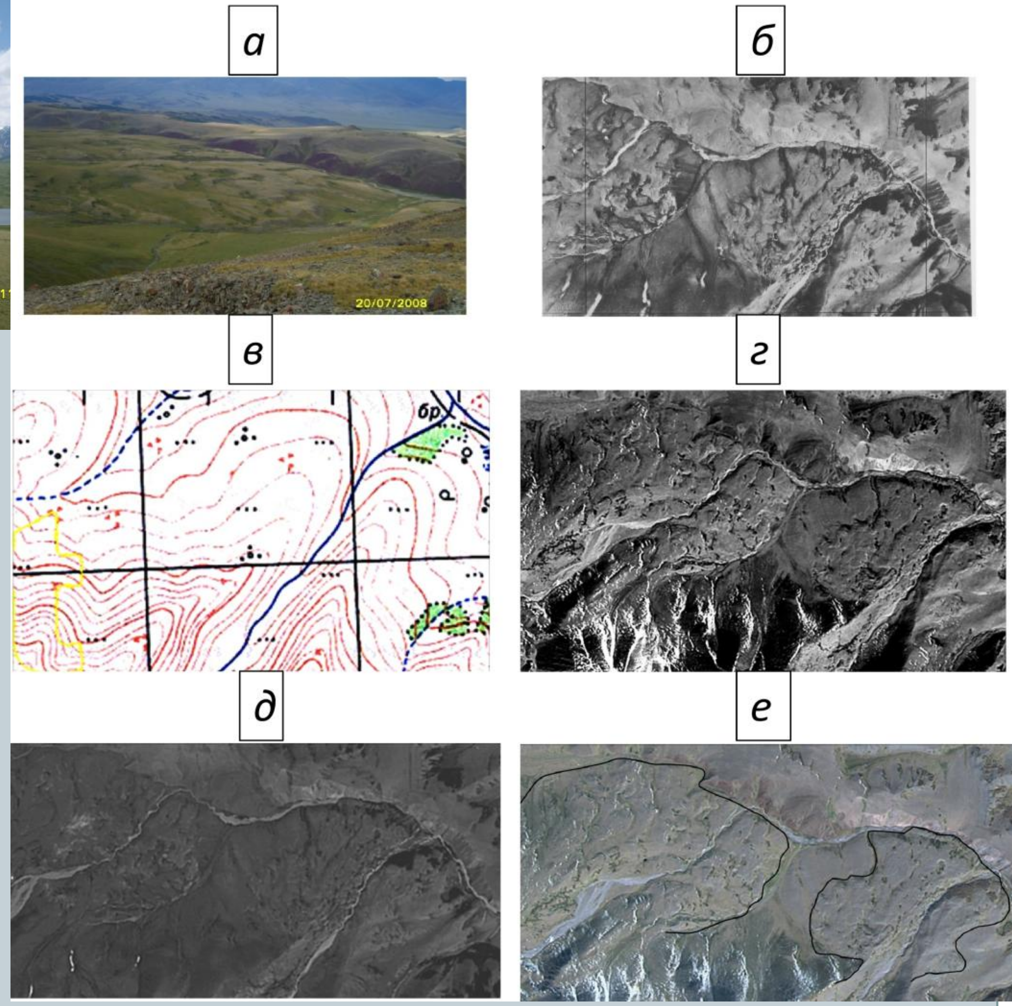

Moraines are composed of a bluish-grey sandy material, having a large number of rounded boulders, mostly granite. Its surface is hummocky-like, with many small, round thermokarst depressions and lakes. These forms are located at the transition from U-shaped valleys to the intermountain depressions, i.e. at altitudes of 1800 – 2200 m *a.s.l.* *Can* be subdivided into several stages: the oldest holds the greatest area but, in some places, the terminal moraines of the youngest stage break through the older ones.

Moraine group II

The moraines of group II are situated within the troughs, reaching 2100 – 2200 m *a.s.l.* at their lowest extension. Their composition is similar to the first group. These are typical moraines of a valley glaciation. The moraines show erosion in many places. Some moraines still dam lakes in the tongue basin, especially the youngest of these moraines. Lateral moraines of this group can be traced on trough shoulders up to the cirques to an altitude of about 2600 – 2700 m *a.s.l.*, but 50 – 150 m below the previous group.

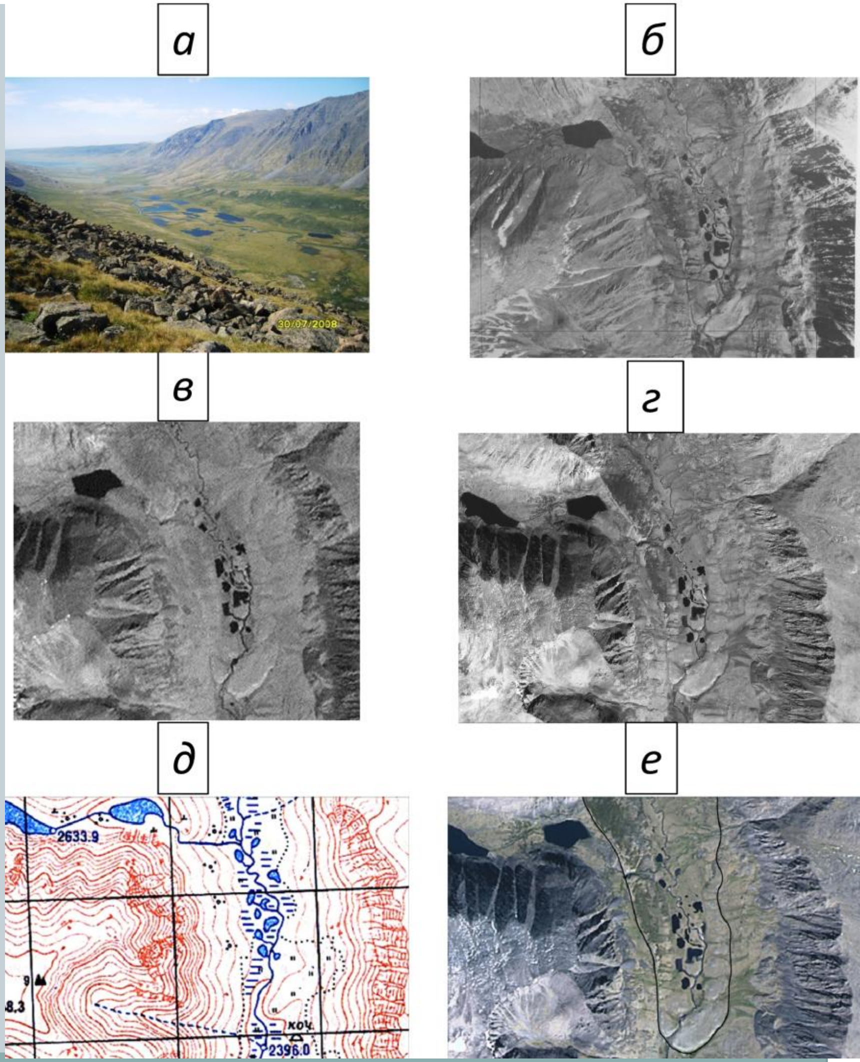

Moraine group III

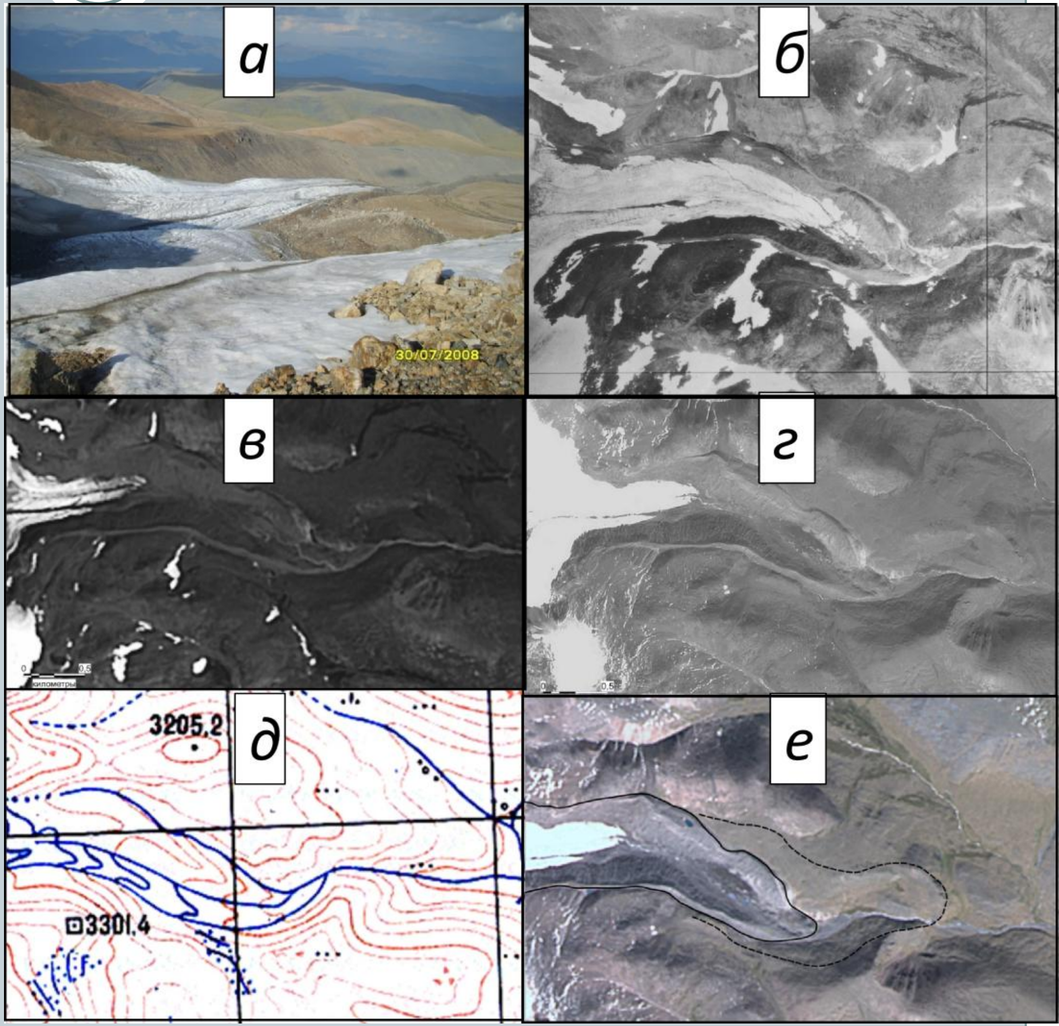

The moraines of group III are characterised by coarse angular stony material intersected with sand and clay deposits. These types of moraines exhibit 3 stages that are usually adjacent to each other or even overlap each other. They mostly form sediment complexes in the upper part of troughs next to the present-day glaciers. These moraine complexes are usually bare of vegetation or slightly covered by pioneer vegetation; they have steep fronts. Glacial ice is sometimes exposed by thermokarst. These moraines are almost unaffected by erosion.

Reconstruction of palaeoglaciation of the Mongun-Taiga massif

. 1: main summit of the massif, 2: mountain ridges and watersheds, 3: rivers, 4: lakes, 5: forested areas, 6: hypothesised extent of glaciers during MIS 4 (based on geomorphic mapping and results given Tables 1 and 2), 7: hypothesised extent of glaciers during MIS 2 (based on geomorphic mapping and dating), 8: LIA glaciers, 9: present-day glaciers. The red frame (inlet) refers to the area plotted in the next slide.

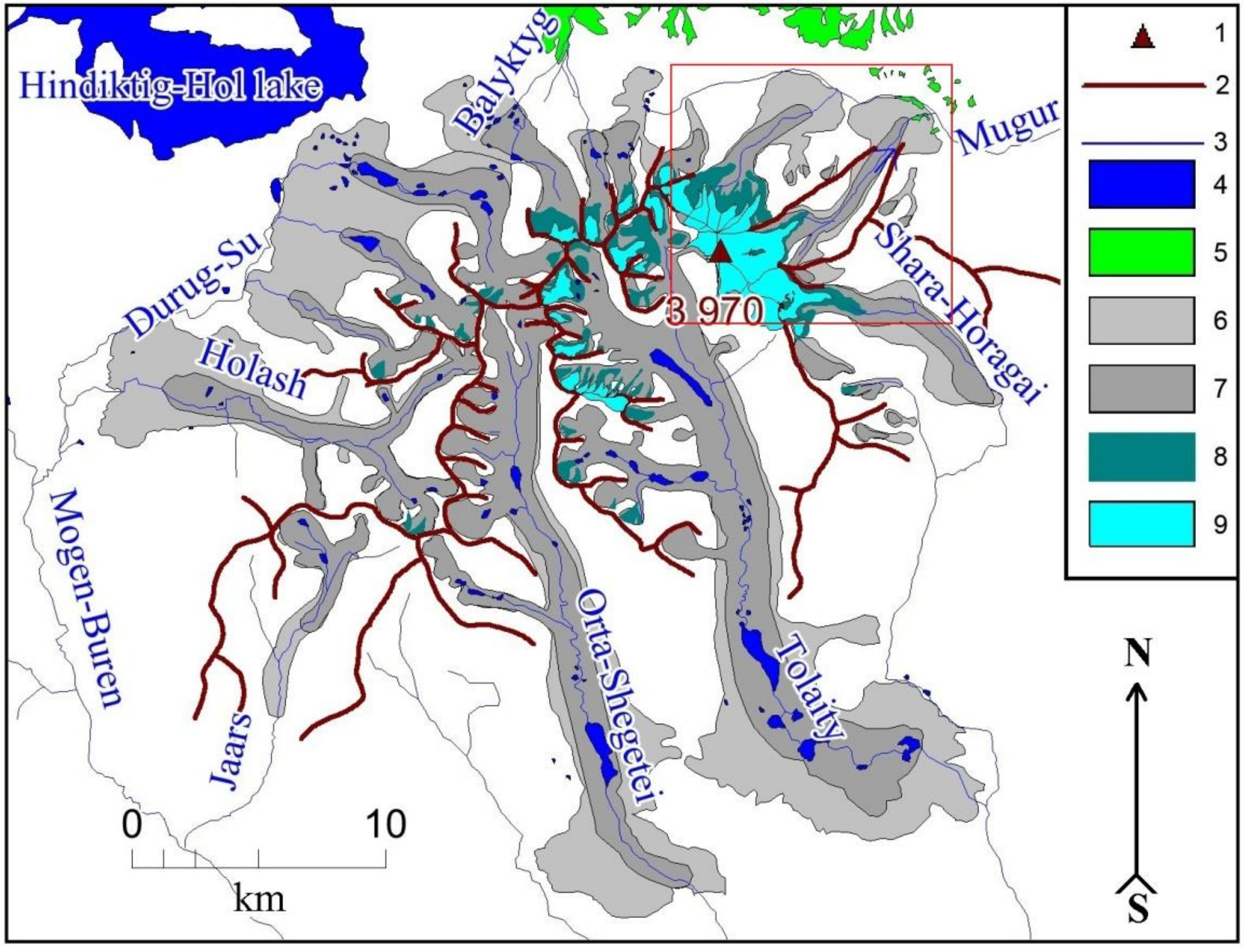

During the maximal advance of the glaciers, their area was 26-times larger than now and the equilibrium line of altitude (ELA) was about 800 m lower.

Relative dating of moraines of the Mongun-Taiga massif. I, II, III correspond to the morphological moraine groups

Moraine group	Number of polygons	N_1/N_2 [1)]	C, % [2)]	B, % [3)]	R [4)]	W, mm [5)]	F, % [6)]	L, % [7)]
I	5	0.20	13.9	73.7 ± 2.50	44.7 ± 1.63	7.0	33.2	56.8
II	5	0.33	7.0	66.3 ± 1.83	40.4 ± 1.80	10.3	32.1	79.2
III	9	0.03	3.3	49.3 ± 1.57	51.3 ± 2.62	4.8	3.7	29.0

[1)] N_1 = the number of boulders having a diameter over 30 cm, N_2 = number of smaller boulders and cobbles

[2)]C = shear-strained boulders; area coverage in %

[3)]B = embedment into finely-grained material,

[4)]R = rebound value (Schmidt-hammer); ± standard error; n (total) = 3708 (110, 229, 3369)

[5)]W = weathering rind thickness (W, mm); ± standard error; n (total) = 76 (10, 15, 51)

[6)]F = proportion of flat-topped boulders

[7)]L = lichen coverage (area coverage given in %),

The rebound values and the weathering rind thicknesses show that the surface of the moraine groups I and II were the most weathered. From a stratigraphic point of view, moraine group I must be older than moraine group II. This trend is best reflected by the parameters C, B and F. Rebound values (R) rapidly decreased during the early stage of moraine evolution.

Main sampling locations on the north-eastern slope of the Mongun-Taiga massif.

Topographic and geomorphic features: 1: main summits of the massif, 2: contour lines, 3: river flow direction, 4: rivers, 5: lakes, 6: present-day glaciers, 7: forested areas, 8: traces of MIS 6 (?) moraines; 9: moraines of group I (hypothesised to be deposited during MIS 4), 10: moraines of group II (hypothesised to be deposited during MIS 2), 11: moraines of group III (neoglacial). Sample categories (sampling site): A: locations of buried wood (1, 2, 3, 4, 5, 6, 7, 14), B: soils (8, 9, 10, 11, 12), C: peat (several sites: 13, 14, 15), and D: boulders.

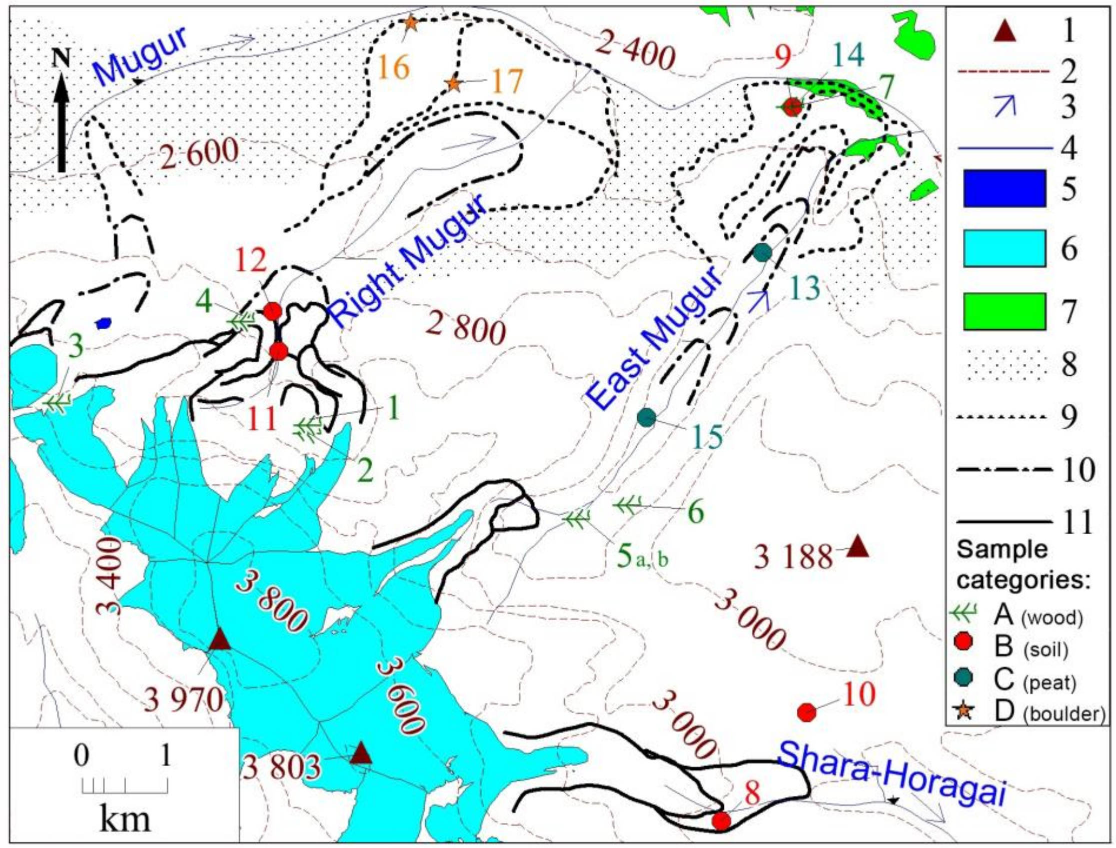

Radiocarbon data from the Mongun-Taiga massif.

Sampling site	Laboratory ID	Altitude (m)	Material	^{14}C age ± error	Calibrated age (1s), cal BP	Climate interpretation	Source
1	LU-3666	2915	wood (A)	57810 ± (≥1820)	c. 60000 – 56000	warm	this paper
2	LU-5822	2965	wood (A)	39300 ± 700	43688 – 42567	warm	this paper
3	KI-912	3300	wood (A)	27500 ± 180	31436 – 31178	warm	(Revushkin, 1974)[1)]
4	KI-913	2800	wood (A)	25100 ± 160	29537 – 28759	warm	(Revushkin, 1974)[1)]
5	SOAN 8116	2700	wood (A)	-	10580 – 10180	warm, humid	(Nazarov et al., 2012)
6	LU-6949	2640	wood (A)	8140 ± 80	9245 – 9000	warm	this paper
5	SOAN 8117	2700	wood (A)	-	6350 – 6170[2)]	warm, humid	(Nazarov et al., 2012)
13	LU-3219	2460	peat (C)	4920 ± 80	5740 – 5588	humid	this paper
8	LU-7283	2960	soil (B)	4860 ± 190	5881 – 5326	warm	this paper
9	LU-5830	2350	charcoal in soil (B)	4570 ± 80	5445 – 5054	warm	this paper
14	LU-6451	2350	peat (C)	4110 ± 100	4819 – 4522	humid	this paper
10	LU-7284	2855	soil (B)	3580 ± 280	4290 – 3515	warm	this paper
7	LU-6452	2350	wood (A)	3370 ± 70	3697 – 3495	warm, humid	this paper
11	LU-8382	2675	soil (B)	2820 ± 150	3141 – 2776	warm	this paper
12	LU-6818	2630	soil (B)	1280 ± 80	1293 – 1089	warm	this paper
15	LU-6817	2535	peat (C)	1190 ± 60	1224 – 1009	warm, moist	this paper

[1)] A $\delta^{13}C$ correction was at that time not performed. A $\delta^{13}C$ value of –25 ‰ was assumed for the correction of the ^{14}C data.

[2)] Original data 10380 ± 200 cal BP

[3)] Original data 6260 ± 90 cal BP

The finding of the ancient wood with cal age 43688 – 42567 BP

Sample properties and ^{10}Be surface ages. Latitude and longitude are in WGS84 coordinates. Shielding correction includes the effects caused by mountain topography, dip and strike of the various boulder surfaces.

Sample name	ETH/UZH label	Latitude (DD)	Longitude (DD)	Elevation (m *a.s.l.*)	Thickness (cm)	Shielding factor	Quartz (g)	Carrier (mg)	^{10}Be content[a] (atoms g^{-1})	Uncertainty ^{10}Be content[b] (atoms g^{-1})	Exposure age[c,e] (a)	Uncertainty[d,e] (+/- a)
16	MIS2	50.337	90.162	2500	3	0.983	20.61	0.35	3.35E+05	1.42E+04	11229	1083 (482)
17	MIS4	50.343	90.154	2408	3	0.947	26.17	0.349	6.33E+05	2.63E+04	23633	2306 (1014)

[a] We used a density of 2.65 g cm^{-3} for all samples.

[b] Uncertainty includes AMS measurements errors and statistical counting error.

[c] We used a rock erosion rate of 1mm/ka

[d] External (internal) uncertainty

[e] Surface exposure ages were calculated with the CRONUS-Earth online calculators (http://hess.ess.washington.edu/, Balco et al., 2008 and version 2.3) and using the scaling scheme for spallation based on Lal (1991)/Stone (2000).

Reconstruction of the vertical fluctuation of the upper treeline ΔF (ΔF^* with tectonic corrections), ELA depression ΔZ_o (ΔZ_o^* with tectonic correction), precipitation *P% (% of the present-day situation)* and temperature difference to the present-day situation ΔT.

Period (and ages of samples of Table 2)	**ΔF (m)**	**ΔF^* (m)**	**ΔZ_0 (m)**	**ΔZ_0^* (m)**	***P%***	**ΔT °C**
			MIS 4			
MIS 4 maximum		– 390	– 800	– 1200	210	– 2.7
MIS 4 stage 2		– 505	– 790	– 1163	105	– 3.5
MIS 4 stage 3		– 465	– 790	– 1145	95	– 3.2
			MIS 3			
56000 – 60000 cal BP	615	309	–	245	100	2.1
43688 – 42567 cal BP	665	470	–	332	100	3.0
31436 – 31178 cal BP	1000	854?	–	458	200	5.9 ?
29537 – 28759 cal BP	500	356	–	102	200	2.5
			MIS 2			
MIS 2 maximum		– 550	658	– 758	46	– 3.8
MIS 2 stage 2		– 536	643	– 731	46	– 3.7
MIS 2 stage 3		– 507	578	– 655	43	– 3.5
MIS 2 stage 4		– 493	523	– 594	43	– 3.4
MIS 2 stage 5		– 478	485	– 551	46	– 3.3
			Holocene			
10580 – 10180 cal BP	400	345	–	84	200	2.4
9245 – 9000 cal BP	340	292		37	200	2.0
6350 – 6170 cal BP	400	367	–	98	200	2.5
5881 – 5326 cal BP		22	–	21	100	0.15
Akkem stage 5326 – 3697 cal BP	–	– 145	151	– 174	110	– 1.0
Interstadial 3697 – 3495 cal BP	50	31	–	2	110	0.2
Historical stage 3495 – 1293 cal BP		– 58	120	– 129	119	– 0.4
Interstadial 1293 – 1009 cal BP		0	0	0	100	0
LIA 1810 – 1820 AD		– 188	120	– 121	73	– 1.3

Reconstruction of temperature fluctuations, precipitation, ELA and the elevation of the upper treeline (with corrections for tectonic uplift).

Red line: temperature, relative to the present-day climate DT* (C); Blue line: precipitation at the current ELA, P (mm); Green line: upper treeline, DF* (m) (relative to present-day elevation); Black line: ELA, DZo * (m) relative to present-day level.

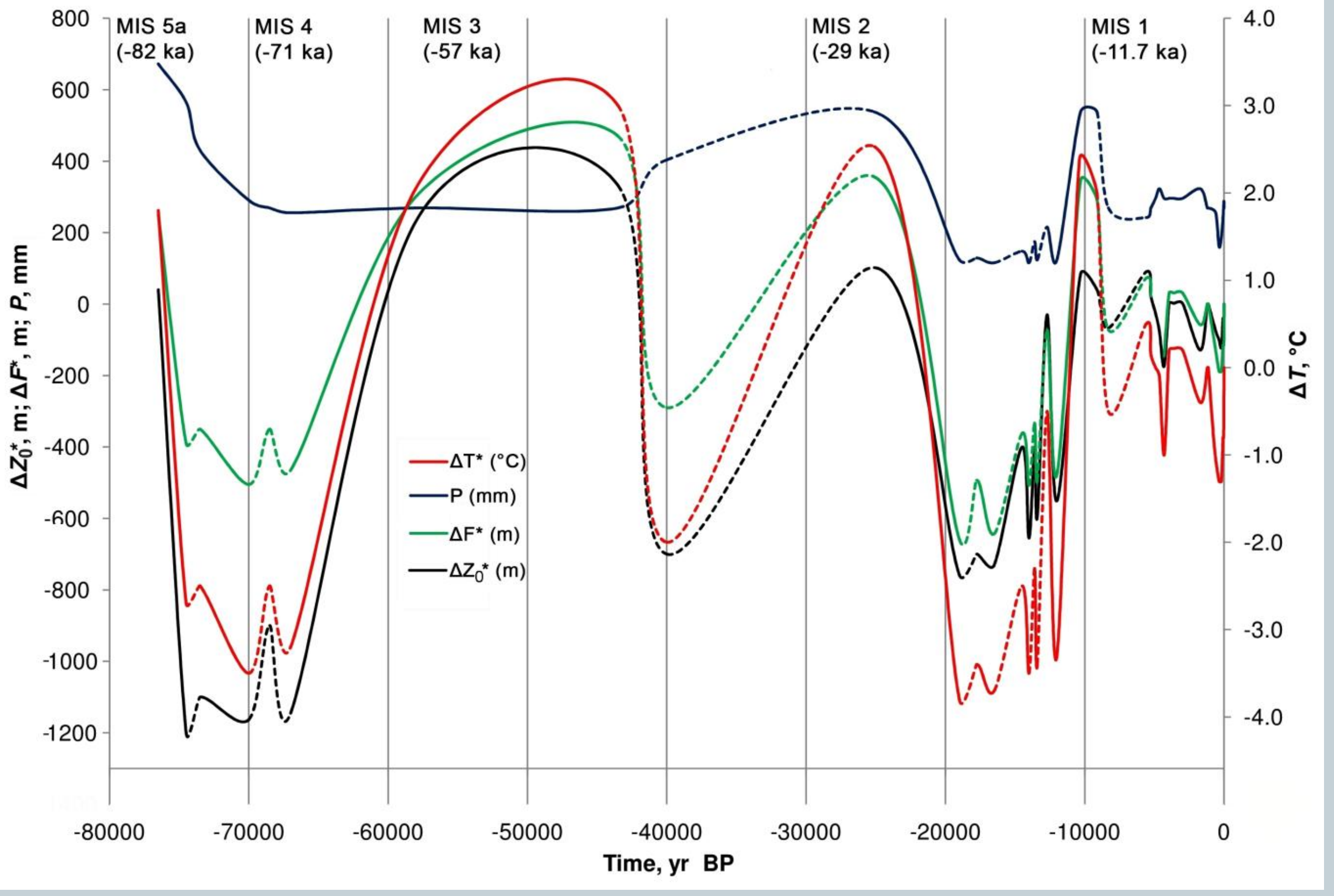

Conclusion

- Using published and our new data, a chronology of glaciation and the reconstruction of climatic fluctuations in the Mongun Taiga (Altai) was rendered possible for the about the last about 80 ka.
- We determined high amplitudes of climatic, glacial and treeline changes. The variability (compared to the present-day climate) of summer temperatures ranged from - 3.8 (- 4.2) to + 3.0 C, precipitation from 43 (37) to 200%, the ELA from e 1200 to 460 m and the upper treeline from - 550 to 470 m.
- The amount of precipitation was the main factor that determined the timing of the maximal glacial advance in Late Pleistocene.
- It seems that the MIS 3c and MIS3a stages were extraordinarily warm. The distinctly elevated treeline during that time evidences that the glaciers retreated to probably high altitudes and covered only a small area. There is no evidence of a complete disappearance of the glaciers even in the warmest periods of the Late Pleistocene.
- The maximum glacier extent was probably during MIS 4. The precise dating of the LGM, however, still remains open and additional 10Be dates (on suitable boulders) are needed.
- During several periods, forest vegetation occupied larger areas than today.
- The actual tendency of warming and increase in precipitation after the LIA maximum probably will lead to a wider expansion of forests.

The article: "Palaeoclimate, glacier and treeline reconstruction based on geomorphic evidences in the Mongun-Taiga massif (south-eastern Russian Altai) during the Late Pleistocene and Holocene" is available:

- https://www.sciencedirect.com/science/article/pii/S1040618217305529
- https://www.researchgate.net/publication/322066644_Palaeoclimate_glacier_and_treeline_reconstruction_based_on_geomorphic_evidences_in_the_Mongun-Taiga_massif_south-eastern_Russian_Altai_during_the_Late_Pleistocene_and_Holocene

Thank You!